Dynamic fault rupture processes of moderate-size earthquakes inferred from the results of kinematic waveform inversion

Takeshi Mikumo
Instituto de Geofisica, Universidad Nacional Autonoma de Mexico, Mexico

Abstract
Several attempts have been made recently to infer the dynamic rupture processes of moderate-size earthquakes from kinematic waveform inversion and dynamic crack inversion. These studies have revealed a quite heterogeneous distribution of dynamic stress drop and relative fault strength over the fault for most earthquakes. In two strike-slip California earthquakes, negative stress drop has been identified in a shallow section of the fault, suggesting the possible existence of a zone of velocity-strengthening frictions. The dynamic models yielded quite short rise times comparable to those inferred from kinematic modelling of observed waveforms. The short slip durations for these earthquakes may probably be attributed to shorter length scale of fault segmentation due to the heterogeneities of shear stress and fault strength.

Key words *dynamic rupture – dynamic stress drop – fault strength – waveform inversion – rise time*

1. Introduction

A number of studies have been made over the last decade to elucidate the complexities of the faulting process of large to moderate-size, inter-plate and intraplate earthquakes. Recent waveform inversion techniques have been applied not only to teleseismic body waves but also to near-source strong ground motions, and revealed heterogeneous slip or moment release distribution and, in some cases, incoherent rupture propagation over the fault. These studies are, however, all based on kinematic fault models including some arbitrary assumptions, and do not involve any dynamic conditions such as the accompanying stress-strain changes on and around the fault.

On the other hand, theoretical and numerical approaches based on spontaneous, dynamic shear crack models (Das and Aki, 1977; Mikumo and Miyatake, 1978; Miyatake, 1980; Das, 1981; Day, 1982; Boatwright and Quin, 1986) indicate that the complex faulting process results mainly from non-uniform shear stress field with heterogeneous fault strength, and partly from local heterogeneities of the crustal structure around the fault zones (Mikumo *et al.*, 1987).

A few attempts have been made to compare the results from waveform inversion with those calculated from dynamic rupture models (Mikumo *et al.*, 1987; Quin, 1990). More recently, a more direct approach has been pursued to recover the dynamic rupture process of moderate-size earthquakes from the previous results of kinematic waveform inversion (Miyatake, 1992a,b, 1993; Mikumo and Miyatake, 1993, 1994; Fukuyama and Mikumo, 1993).

The main purpose of the present paper is to

summarize the above approach, to review some of the results obtained to date, and to discuss their implications and remaining problems.

2. Method

Up to the present, the following two approaches have been developed to recover the dynamic rupture process of actual earthquakes. Since these approaches here are based on the results from, or directly incorporate, kinematic waveform inversion, we briefly describe the method of kinematic inversion.

1) *Kinematic waveform inversion* – Although there are several inversion techniques, we refer only to the results from non-linear inversion that solved simultaneously both slip and rupture time (*e.g.* Takeo, 1987; Hartzell, 1989; Fukuyama, 1991), since the mode of rupture propagation is not known a priori and since the rupture time has a strongly non-linear effect on the waveforms. This may be reasonable because rupture propagation could be non-uniform on a heterogeneous fault under inhomogeneous stress field, as suggested by dynamic shear crack models.

In the waveform inversion, Green's functions are calculated for each combination of individual subfaults and stations by using the discrete wave number or DWFE method for a horizontally layered structure appropriate to the source region. The synthetic seismograms are then constructed by convolving these Green's functions with an assumed slip or slip-velocity source time function and by integrating them over the entire fault surface. An application of iterative least squares, which minimizes the square sum of the difference between the recorded and synthetic waveforms, provides estimates of two model parameters, *i.e.* the slip and rupture starting time on each of the subfaults.

2) *Inversion from kinematic fault model to dynamic rupture model* – The controlling factors governing dynamic fault rupture process during earthquakes are the initial shear stress σ_0, sliding frictional stress σ_d, and fault

strength or the peak shear stress σ_s (*e.g.* Mikumo and Miyatake, 1978; Miyatake, 1980; Das, 1981). The aim of the studies cited above is to derive the spatial distribution of dynamic stress drop (the difference between the initial shear stress and sliding frictional stress $\sigma_0 - \sigma_d$) and strength excess (the difference between the peak shear stress and initial stress $\sigma_s - \sigma_0$), from the distribution of fault slips and rupture starting times obtained from the kinematic waveform inversion.

A – The first approach, which follows the method developed mainly by Miyatake (1992a), uses the previous results from kinematic waveform inversion, including the following three steps.

1) The first step is to construct a 3-D dynamic rupture model which incorporates a vertical strike-slip fault (Mikumo *et al.*, 1987) or a dipping thrust or normal fault (Mikumo and Miyatake, 1993) embedded in a horizontally layered velocity structure appropriate to the source region. The geometry of the fault plane is taken as the same as in the kinematic model. In order to calculate dynamic ruptures propagating spontaneously over the fault, the wave equations in the 3-D space are solved numerically by a finite difference scheme under appropriate boundary conditions and a critical stress fracture criterion.

2) The second step is to estimate the relative fault strength at each grid point on the fault. To do this, the rupture time at this point during rupture propagation is fixed to the time obtained from the waveform inversion (Miyatake, 1992a). This means that the dynamic rupture remains locked before this time and the shear stress increases up to this time. The peak shear stress just before rupturing this point may be regarded as the relative fault strength. The strength excess is defined as the difference between the estimated peak shear stress and the assumed initial stress. However, these values are dependent on the grid spacing and the time increment used in numerical calculations and hence should be regarded as a lower limit of their real values.

3) The third step is to estimate the dynamic stress drop from the kinematic fault slip. Two

different techniques have been proposed for this purpose. a) A straightforward way is to apply a linear inversion to calculate static stress drop at each grid point directly from the final fault slip, by solving the equilibrium equations combined with some boundary conditions in the 3-D space (Miyatake, 1992a). The obtained local static stress drop has been adjusted to some extent in calculating dynamic rupture propagation. b) An alternative one is to apply a non-linear iterative inversion. First, slip distribution is calculated from a starting dynamic model with a uniform strength and sliding frictional stress under a homogeneous stress field, and compared with the kinematic fault slip. At the next iteration, the ratio between the kinematic and dynamic slips on each of the subfaults is then multiplied to the initially assumed stress drop there, and the dynamic slips are again calculated. This procedure is repeated several times to minimize the square sum of the difference between the kinematic and dynamic slips, and a best fitting distribution of dynamic stress drop is estimated (Mikumo and Miyatake, 1993).

B – The second approach involves an alternate application of the waveform inversion and kinematic-dynamic inversion (Fukuyama and Mikumo, 1993), to obtain a best fit between the recorded and synthetic seismograms. In this case, the first step is to calculate dynamic rupture propagation for a homogeneous strength under a uniform shear stress, yielding the slip source time functions with different rise times, final slips and rupture times on each of the subfaults. These are used as starting model parameters in the initial kinematic waveform inversion. The kinematic inversion is performed as described in (1), and then the kinematic-dynamic inversion is applied following the three steps given in (2). These two inversions are repeated several times until the overall residual between the recorded and synthetic waveforms becomes reasonably small. This type of approach could start with the kinematic waveform inversion, rather than using an initial dynamic model.

A more straightforward approach is being attempted through numerical experiments for the retrieval of dynamic source parameters directly from observed waveforms with a generalized non-linear inversion (Horikawa and Hirahara, 1993).

3. Results

In this section, the results obtained to date are reviewed and discussed to focus our attention on the heterogeneous properties of fault strength and dynamic stress drops, and to where the dynamic rupture initiates and how it propagates under these environments.

3.1. *Strike-slip earthquakes in California*

Two strike-slip earthquakes have been investigated by applying the above method.

a) The first case is the 1979 Imperial Valley earthquake ($M = 6.5$), for which the slip and rupture time distribution has been estimated from kinematic waveform inversion. The results (Archuleta, 1984) show that the region of maximum slip is concentrated at depths around 10 km and that the rupture velocity is highly variable, in one region exceeding the P-wave velocity. Quin (1990) attempted to simulate the kinematic results by generating more than 200 dynamic models, and estimated dynamic stress drop and strength excess. His final model suggested some depth dependence of the stress drop including negative values at depths down to 7 km. Miyatake (1992a) also obtained the distribution of dynamic stress drop and strength excess by the method described above, which satisfactorily reproduces the kinematic fault slip, slip rates and rupture times. However, since he imposed a non-negative stress drop condition in deriving static stress drop, no negative dynamic stress drop has been detected unlike the results suggested by Quin (1990). The rise times in his dynamic model range between 0.5 and 1.5 s, which are close to that assumed in the kinematic model.

The dynamic rupture initiated at the southern deep fault section having low strength excess, breaking a medium-size zone with a mod-

erate stress drop of 40 bars, then broke a large-size zone with a high stress drop of 80 bars, and was decelerated near the northern edge of the fault where high strength and low stress drop have been detected.

b) The second one is the 1984 Morgan Hill, California earthquake ($M = 6.2$) that occurred on the Calaveras fault, for which two different kinematic waveform inversions have been performed. Beroza and Spudich (1988) detected extremely heterogeneous slip distribution with very low slip at shallower fault sections, delayed rupture at a small section, together with an unusually short rise time of 0.2 s. The dynamic rupture process of this earthquake was investigated by Mikumo and Miyatake (1994). The distribution of static and dynamic stress drops has been estimated independently, and found to be essentially similar but with slightly larger values for the static case. It was found from the best-fitting model that high slips in two deep fault sections located at 8-12 km come from local dynamic stress drop exceeding 140 bars and 40 bars, respectively (fig. 1). Negative stress drops down to −15 bars are required to explain very low slip over the shallow fault section. If a non-negative stress drop constraint is imposed, somewhat larger fault slips are obtained there than those estimated from the kinematic inversion. The strength excess is found to be generally small, except at the small section that has delayed rupture propagation. The dynamic model yielded the slip-rate functions with rise times ranging between 0.2 and 0.5 s, which is very close to that assumed in the kinematic model (Mikumo and Miyatake, 1994).

The dynamic rupture started from a small nucleus zone with a small stress drop, propagated southeastwards breaking the deeper fault section with moderate stress drops, and broke a relatively high strength zone after a short time of arrest, with the highest stress drop.

3.2. *Strike-slip earthquakes in Central Japan*

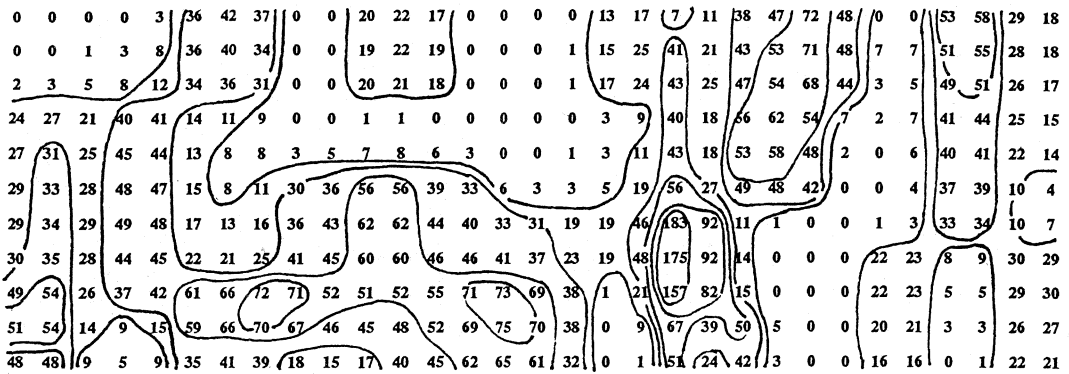Five strike-slip earthquakes in Central Japan have been investigated.

a) The earthquakes investigated were the 1974 ($M = 6.9$), and the 1980 Off-Izu peninsula ($M = 6.7$) earthquakes that occurred close to the boundary between the Philippine Sea and Eurasian plates, and two inland earthquakes, the 1969 Gifu ($M = 6.6$) and the 1984 Western Nagano ($M = 6.8$) earthquakes in Central Japan. The kinematic waveform inversion provided quite heterogeneous slip and incoherent rupture propagation (Takeo, 1987, 1988; Takeo and Mikami, 1987, 1990). The spatial distribution of dynamic stress drop and strength excess on the faults of these earthquakes have been investigated in detail by Miyatake (1992b), by applying the techniques mentioned before (fig. 2a,b).

In the two Off-Izu peninsula earthquakes, the dynamic rupture initiated with a high stress drop of 120-180 bars, near the central bottom section of the fault where the strength excess is quite low, and propagated bilaterally and upwards to high strength zones with decelerated velocities. The rupture finally broke these high strength zones with moderate (1974) to high (1980) stress drop ranging between 40 and 100 bars. The distribution of high stress drop and high strength excess appears complementary.
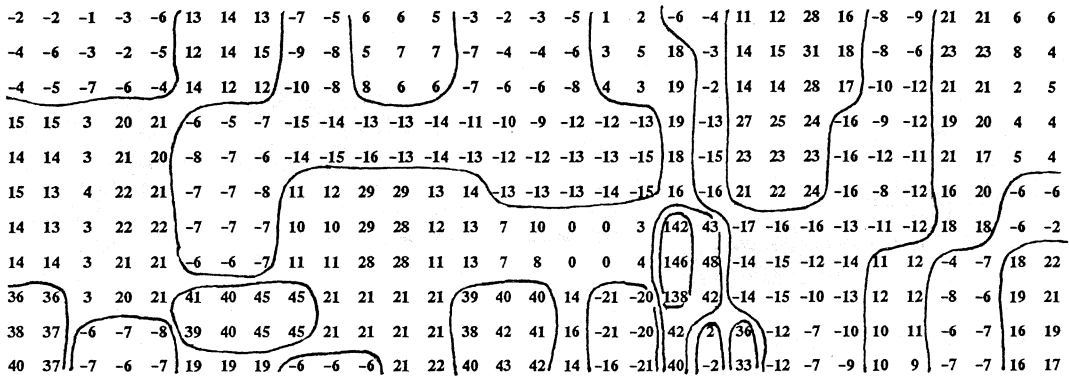
The two inland earthquakes, on the other hand, have more heterogeneous features in dynamic rupture process. Generally, the rupture initiated with low stress drop from a central shallow fault section having low strength excess, and then propagated downwards and bilaterally. For the 1969 earthquake, the rupture broke low to moderate strength zones at mid-depths with a high stress drop of 80 bars, while the 1984 earthquake ruptured two separate, moderate-strength zones at shallow to mid-depths, with high stress drops of 120-160 bars. No negative stress drop was identified in the four earthquakes, because a non-negative constraint was imposed. The rise time in the slip-rate functions has not been discussed.

b) Another one investigated was the 1990 Izu-Oshima earthquake ($M = 6.5$) that occurred quite close to the 1980 Off-Izu peninsula earthquake. For this earthquake, an iterative, kinematic waveform inversion and dynamic crack inversion were applied alternately to obtain a

Dynamic Slip

```
 0   0   0   0   3  36  42  37   0   0  20  22  17   0   0   0   0  13  17   7  11  38  47  72  48   0   0  53  58  29  18
 0   0   1   3   8  36  40  34   0   0  19  22  19   0   0   0   1  15  25  41  21  43  53  71  48   7   7  51  55  28  18
 2   3   5   8  12  34  36  31   0   0  20  21  18   0   0   0   1  17  24  43  25  47  54  68  44   3   5  49  51  26  17
24  27  21  40  41  14  11   9   0   0   1   1   0   0   0   0   0   3   9  40  18  56  62  54   7   2   7  41  44  25  15
27  31  25  45  44  13   8   8   3   5   7   8   6   3   0   0   1   3  11  43  18  53  58  48   2   0   6  40  41  22  14
29  33  28  48  47  15  11  30  36  56  56  39  33   6   3   3   5  19  56  27  49  48  42   0   0   4  37  39  10   4
29  34  29  49  48  17  13  16  36  43  62  62  44  40  33  31  19  19  46  83  92  11   1   0   0   1   3  33  34  10   7
30  35  28  44  45  22  21  25  41  45  60  60  46  46  41  37  23  19  48 175  92  14   0   0   0  22  23   8   9  30  29
49  54  26  37  42  61  66  72  71  52  51  52  55  71  73  69  38   1  21 157  82  15   0   0   0  22  23   5   5  29  30
51  54  14   9  15  59  66  70  67  46  45  48  52  69  75  70  38   0   9  67  39  50   5   0   0  20  21   3   3  26  27
48  48   9   5   9  35  41  39  18  15  17  40  45  62  65  61  32   0   1  51  24  42   3   0   0  16  16   0   1  22  21
```

Dynamic Stress Drop

```
-2  -2  -1  -3  -6  13  14  13  -7  -5   6   6   5  -3  -2  -3  -5   1   2  -6  -4  11  12  28  16  -8  -9  21  21   6   6
-4  -6  -3  -2  -5  12  14  15  -9  -8   5   7   7  -7  -4  -4  -6   3   5  18  -3  14  15  31  18  -8  -6  23  23   8   4
-4  -5  -7  -6  -4  14  12  12 -10  -8   8   6   6  -7  -6  -6  -8   4   3  19  -2  14  14  28  17 -10 -12  21  21   2   5
15  15   3  20  21  -6  -5  -7 -15 -14 -13 -13 -14 -11 -10  -9 -12 -12 -13  19 -13  27  25  24 -16  -9 -12  19  20   4   4
14  14   3  21  20  -8  -7  -6 -14 -15 -16 -13 -14 -13 -12 -12 -13 -13 -15  18 -15  23  23  23 -16 -12 -11  21  17   5   4
15  13   4  22  21  -7  -7  -8  11  12  29  29  13  14 -13 -13 -13 -14 -15  16 -16  21  22  24 -16  -8 -12  16  20  -6  -6
14  13   3  22  22  -7  -7  -7  10  10  29  28  12  13   7  10   0   0   3 142  43 -17 -16 -16 -13 -11 -12  18  18  -6  -2
14  14   3  21  21  -6  -6  -7  11  11  28  28  11  13   7   8   0   0   4 146  48 -14 -15 -12 -14  11  12  -4  -7  18  22
36  36   3  20  21  41  40  45  45  21  21  21  21  39  40  40  14 -21 -20 138  42 -14 -15 -10 -13  12  12  -8  -6  19  21
38  37  -6  -7  -8  39  40  45  45  21  21  21  21  38  42  41  16 -21 -20  42   2  36 -12  -7 -10  10  11  -6  -7  16  19
40  37  -7  -6  -7  19  19  19  -6  -6  -6  21  22  40  43  42  14 -16 -21  40  -2  33 -12  -7  -9  10   9  -7  -7  16  17
```

Strength Excess

```
0  0  0  0  1  1  1  0  0  0  0  0  0  1  0  0  1  1  1  1  1  1  1  0  0  0  1  0  0  0  1  0  0
0  0  1  0  1  1  2  0  0  0  0  1  1  1  0  1  1  1  1  0  5  1  3  4  6  3  1  1  3  2  0
1  1  1  1  2  1  0  0  0  0  0  1  1  1  1  1  1  0  0  0  2  1  4  4  8  2  1  1  2  1  0
0  0  0  2  1  0  0  0  0  1  1  2  2  2  2  1  1  0  0  0  1  2  7  4  7  0  1  1  6  2  0
1  1  1  2  0  0  0  0  0  1  2  3  3  3  1  1  0  0  0  0  0  2  6  5  4  0  0  0  4  2  1
1  1  1  2  0  0  0  0  0  1  4  7  5  3  0  0  0  0  1  5  0  0  4  4  1  0  0  0  3  1  0
2  0  1  2  0  8  0  0  0  2  3  7  4  2  0  0  0  0  2  4  5  0  0  4  0  0  1  1  2  0  0
2  0  1  3  0  8  0  0  0  1  3  5  4  1  0  0  2  0  1  6  15  0  0  5  0  0  2  1  0  0  1
4  1  2  0  0  0  1  0  0  0  3  2  3  2  1  3  3  0  0  7  17  0  0  4  1  0  2  0  1  0  1
4  3  2  0  1  1  3  0  0  0  5  4  3  5  2  1  5  0  0  2  0  0  2  2  2  1  2  2  0  1  1
4  3  1  0  2  2  2  0  0  2  7  3  1  5  5  3  6  0  0  1  3  0  3  1  2  2  2  2  1  1  1
```
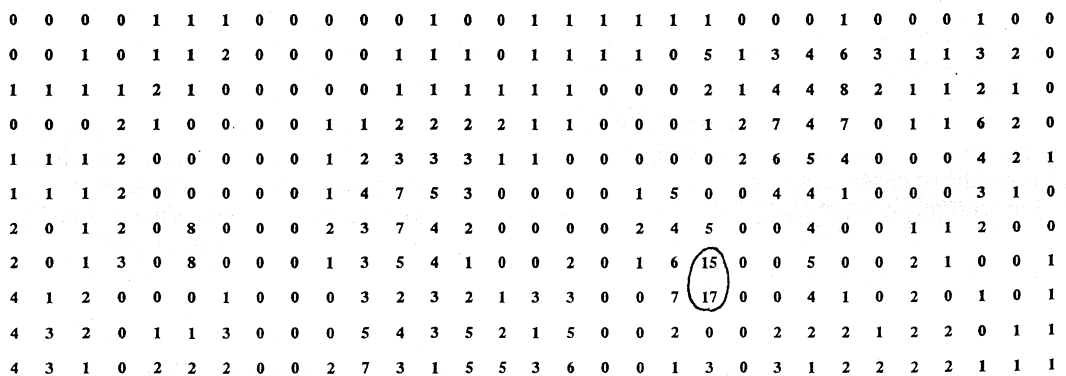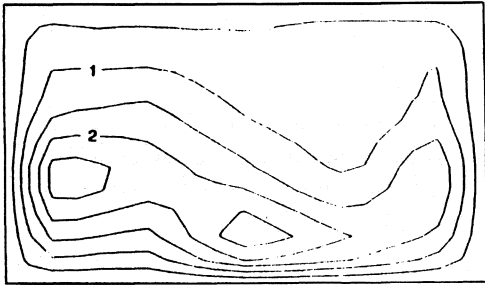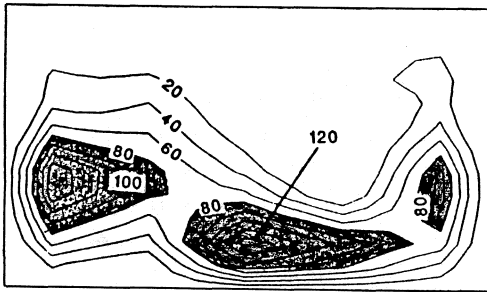
Fig. 1. Distribution of dynamic slip, dynamic stress drop and strength excess in model II (negative stress drop model) for the 1984 Morgan Hill, California earthquake (Mikumo and Miyatake, 1994).
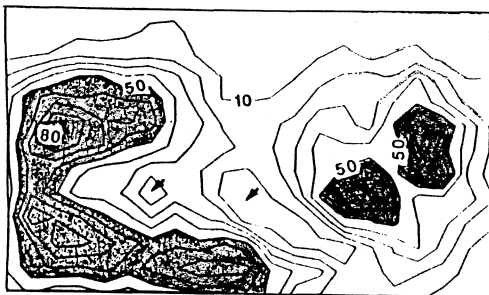
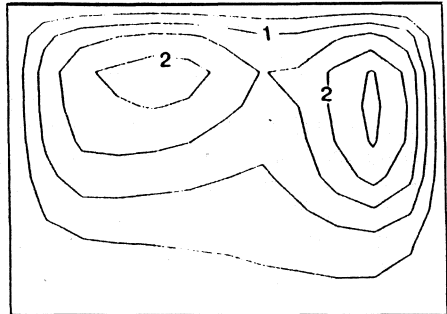(a)

The 1980 Izu-Hanto-Toho-Oki Earthquake (M=6.7)

(b)

The 1984 Western-Nagano Earthquake (M=6.8)

Dynamic Model Slip (m)

Dynamic Model Slip (m)

Stress Drop (bars)

Stress Drop (bars)

Strength Excess (bars)

Strength Excess (bars)

Fig. 2a,b. Distribution of dynamic slip, dynamic stress drop and strength excess: a) for the 1980 Off-Izu peninsular earthquake (Miyatake, 1992b); b) for the 1984 Western Nagano earthquake (Miyatake, 1992b).

better fit between the recorded and synthetic waveforms (Fukuyama and Mikumo, 1993), following the procedure described in Section 2 (2) B. This procedure yielded not only the distribution of fault slips and rupture times but also that of dynamic stress drop and strength excess simultaneously. The results show that a large slip with a maximum of 130 cm is concentrated around the initiation point of rupture located at a shallow depth near the northern edge of the fault, while the adjacent zone south of this point has quite low slips and delayed rupture times. This means that the dynamic rupture initiated with moderate dynamic stress drop of 35 bars at the nucleus zone having low strength excess and was encountered with a high strength region located just south of the hypocentral zone. The decelerated rupture then broke this region with a quite low stress drop, and propagated nearly unilaterally with a low stress drop over low strength zones towards the southern edge of the fault. These patterns of rupture propagation appear quite similar to those of the two Off-Izu earthquakes. No negative stress drop was detected. The rise time of the source time function was found to be rather short at the hypocentral zone and at the deeper fault sections but somewhat extended at the region south of the hypocentral zone.

3.3. *A thrust-type earthquake in Central Japan*

An example of the thrust-type earthquakes investigated is the 1961 Kita-Mino earthquake ($M = 7.0$) that occurred in the inland region of Central Japan. Heterogeneous slip distribution and non-uniform rupture propagation were detected from the kinematic waveform inversion also for this earthquake (Takeo and Mikami, 1990). To solve the spontaneous, dynamic rupture problem for thrust-type earthquakes, the wave equations for a 3-D space were solved for all points located above and below a dipping fault, with specific boundary conditions along and across the fault (Mikumo and Miyatake, 1993). It was found that the dynamic rupture gives appreciably larger fault slips on the hanging wall side than on the foot wall side. The results show strongly heterogeneous distribution of the dynamic stress drop and strength excess, indicating both lateral and depth variations, but no negative stress drop was detected (fig. 3).

The rupture of this earthquake initiated, with a low stress drop, at a small low strength nucleus zone at mid-depth, then broke the shallower and deeper fault sections having moderate strength, with relatively high stress drop of 50-60 bars, and finally overcame high strength zones located at the central bottom and the SW shallow fault sections. The rise times calculated from the dynamic model range mainly between 1.0 and 3.0 s, which are comparable to those assumed in the kinematic model.

3.4. *Other earthquakes*

Recently, Miyatake (1993) estimated the spatial distribution of dynamic stress drop from the fault slip derived from the kinematic waveform inversion also for several large to moderate-size earthquakes; the 1978 Tabas ($M_s = 7.4$), 1981 Playa Azul ($M_s = 7.3$), 1985 Michoacan ($M_s = 8.1$), and 1986 North Palm Spring ($M = 5.9$) earthquakes. In these earthquakes, however, the distribution of strength excess was not obtained, since a constant rupture velocity was assumed in the waveform inversion. The dynamic rupture process of the 1993 Off-Hokkaido earthquake, Japan, was also studied by Ide and Takeo (1994).

4. Discussion

4.1. *The distribution of dynamic stress drop and strength excess*

The distribution of dynamic stress drop and strength excess was obtained as described above for several moderate-size earthquakes. The above results indicate four different zones of the distribution:
  1) low stress drop on a low strength zone;
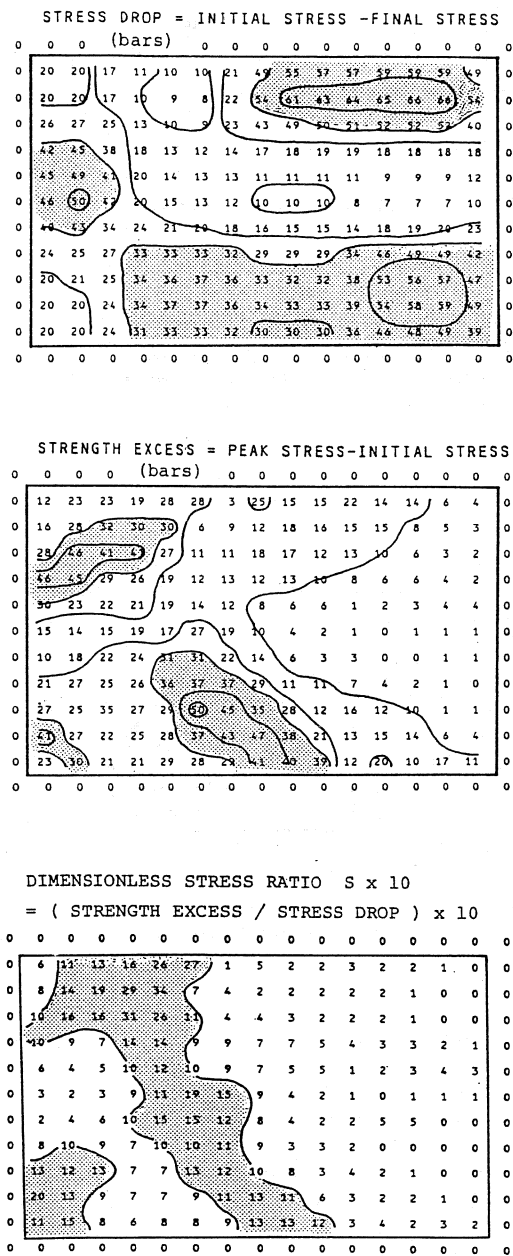 2) high stress drop on a low strength zone;

1961 Kita-Mino Earthquake

STRESS DROP = INITIAL STRESS −FINAL STRESS
(bars)

STRENGTH EXCESS = PEAK STRESS−INITIAL STRESS
(bars)

DIMENSIONLESS STRESS RATIO S x 10
= (STRENGTH EXCESS / STRESS DROP) x 10

Fig. 3. Distribution of dynamic stress drop, strength excess and a dimensionless stress factor S for the 1961 Kita-Mino earthquake (Mikumo and Miyatake, 1993).

3) high stress drop on a high strength zone;
4) low stress drop on a high strength zone.

The above three zones (2), (3) and (4) were defined (Miyatake, 1992b) as a «weak asperity», a «strong asperity» and a «barrier», respectively.

These zones may also be characterized by a «dimensionless stress ratio» S (Das and Aki, 1977), which is the ratio of the strength excess to the dynamic stress drop. The above classifications given in table I are used here as only a relative sense but may be a good indication for the type of fault ruptures. For smaller S values corresponding to zone (2), it is easier for the rupture to initiate at and propagate smoothly over asperities, while larger S values corresponding to zone (4) provide stronger resistance to rupture propagation and hence work as barriers (Mikumo and Miyatake, 1993). Actually, these patterns are well identified in the two published papers. In the case of the 1961 Kita-Mino earthquake (fig. 3) (Mikumo and Miyatake, 1993), there is a wide zone with low strength excess which includes the rupture initiation point, and a barrier zone with large S values extending obliquely from the shallow to deep sections of the fault, which decelerated rupture propagation. For the 1990 Izu-Oshima earthquake (Fukuyama and Mikumo, 1993), small S values coming from low strength excess and high stress drop can be identified in the nucleus zone, while a zone of large S values exists just adjacent to the nucleus zone (the figure not shown here).

The initiation and propagation of dynamic rupture for the earthquakes studied here indicate two different types. In all cases, the rupture initiates at a nucleus zone with low strength excess. This implies that the tectonic stress around there had reached marginally the level of the shear strength of the fault just before the earthquake. However, the first type initiated with a low stress drop at the nucleus zone (zone 1), then propagated over weak asperities (zone 2) and broke strong asperity zones (zone 3) or sometimes barrier zones (zone 4). The other one initiated with a quite high stress drop at a weak asperity zone (zone 2) and then propagated over strong as-

Table I. Distribution patterns of the dynamic stress drop and strength excess.

Zone	Stress drop/Strength excess	S	Type
1	*Low stress drop* Low strength zone	uncertain	
2	*High stress drop* Low strength zone	small	weak asperity
3	*High stress drop* High strength zone	moderate	strong asperity
4	*Low stress drop* High strength zone	large	barrier

$S = (\sigma_s - \sigma_0) / (\sigma_0 - \sigma_d)$.
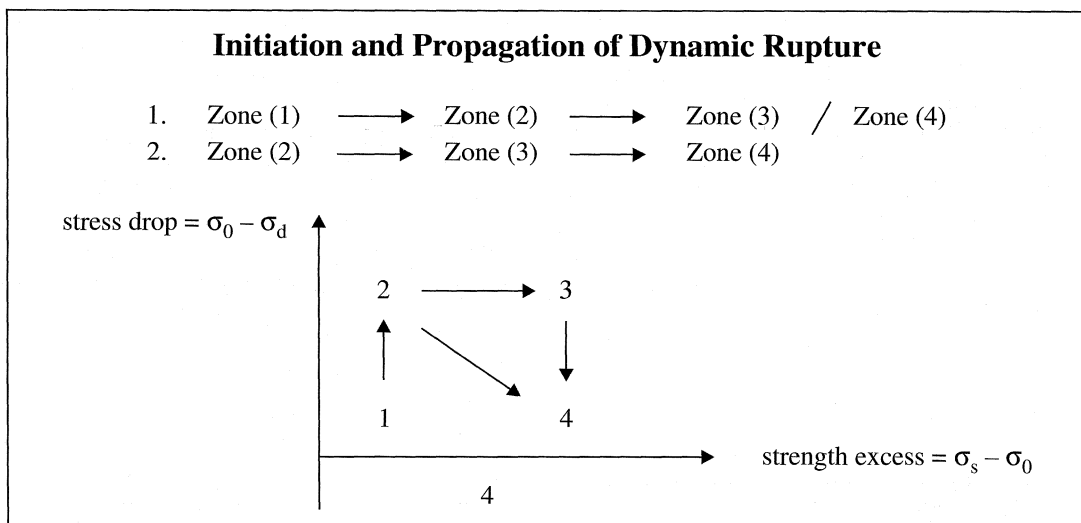
Fig. 4. Mode of initiation and propagation of dynamic rupture with respect to the dynamic stress drop and strength excess.

perity zones (zone 3). These patterns are described in fig. 4.

4.2. *Implications of negative stress drop*

As mentioned before, negative dynamic stress drop was detected over shallow fault sections in two California earthquakes of strike-slip type, if we refer to the results of Quin (1990) for the 1979 Imperial Valley earthquake instead of Miyatake's (1992a).

The possible existence of negative stress drop suggests that there could be a zone of velocity-strengthening frictional behavior in the shallow fault sections. Recent laboratory ex-

periments (*e.g.* Stesky, 1978; Blanpied *et al.*, 1991) show that the frictional sliding behavior changes from velocity-weakening to velocity-strengthening at temperatures above 300-350 ℃. It has also been suggested (Marone and Scholz, 1988; Scholz, 1990) that the sedimentary layers existing in a very shallow portion of the crust may involve thick unconsolidated fault gouge materials which could indicate velocity-strengthening or a negative stress drop. This would be expected at depths shallower that 2-3 km, while the temperature-dependent behavior would occur at depths probably deeper than 8-10 km (Mikumo, 1992). The two California earthquakes suggest different depth ranges for possible negative stress drop; one covers almost the entire fault section shallower than 6-7 km, and the other covers a part of the fault section shallower than 6 km and intervenes into a deeper section down to 12 km. Accordingly, it may be premature to distinguish which explanation would be more appropriate to the present case. One plausible explanation would be that there could be patched zones of unconsolidated fault gouge or high temperatures at these depths (Mikumo and Miyatake, 1994b).

4.3. *Rise times and their implications to fault mechanics*

As described before, new attempts have been made to recover the dynamic rupture processes of earthquakes through kinematic waveform inversion and dynamic crack inversion, and revealed the spatial distribution of dynamic stress drop and relative fault strength for several moderate-size earthquakes. However, there still remains a problem to be solved in the results obtained from the first approach (A), as to how well the dynamic rupture models derived could reproduce the recorded waveforms. This is because the form of the source time function or the rise time in all kinematic models was assumed to be constant everywhere on the fault, although this is not reasonable from a dynamic point of view. Dynamic ruptures, on the other hand, yield different slip functions with the rise times depending on the

dynamic stress drop and fault strength and hence varying with the location of the fault.

For some of the earthquakes investigated (1979 Imperial Valley and 1984 Morgan Hill earthquakes), it has been shown (Miyatake, 1992a; Mikumo and Miyatake, 1994) that the rise times calculated from the dynamic models are very close to those assumed in the corresponding kinematic fault models. This leads to the possibility that the dynamic models could reproduce the recorded waveforms, although the corresponding synthetic seismograms have not been calculated.

For the above reasons, the alternative approach (B) (Fukuyama and Mikumo, 1993) may be more promising to obtain a best fit between the recorded and synthetic waveforms by applying kinematic waveform inversion and dynamic crack inversion alternately. In the case of the 1990 Izu-Oshima earthquake, the fit in the final model was much improved over that in the starting model, but there still remain some discrepancies. The reason for this may be due to the effects from more complicated, laterally heterogeneous crustal structure around the source region than assumed in this study.

The Morgan Hill, California earthquake indicated extremely heterogeneous distribution of dynamic stress drop even with negative values, and generated very short rise times of 0.2-0.5 s (fig. 5) (Mikumo and Miyatake, 1994). Preliminary calculations (Mikumo and Beroza, 1994) show that the synthetic seismograms derived from the dynamic rupture model incorporating the above slip-velocity functions are nearly consistent with the recorded waveforms. More refined models are now being constructed to obtain a better fit between the synthetic and recorded waveforms.

If this is indeed the case, the shorter rise times have important implications on sliding frictional behaviors on the fault surface under realistic environments. It has long been discussed and explicitly pointed out (Heaton, 1990) that the rise times derived from kinematic modeling of ground motion data are much shorter than those expected from the overall rupture duration on the fault and expected from dynamic shear crack models. The short slip duration appears to be supported also
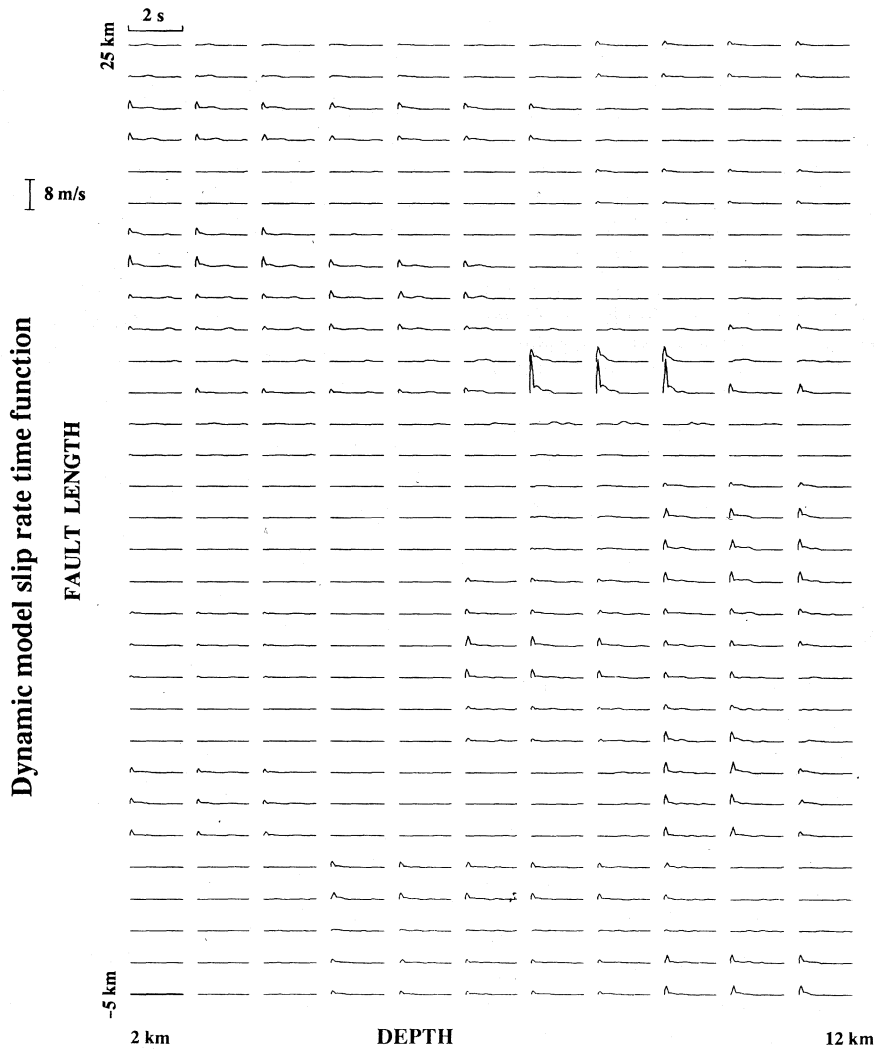
Fig. 5. Distribution of the slip-rate functions on the fault in model II (negative stress drop model) (Mikumo and Miyatake, 1994).

by field evidence (Yomogida and Nakata, 1994). To reconcile the above discrepancy, Heaton (1990) introduced a simple slip-rate dependent friction law, which would produce a self-healing pulse of slip propagating over the fault. Actually a two-dimensional faulting simulation incorporating the simplified rate-dependent friction law (Cochard and Madariaga,

1994) could produce the short duration rupture pulses suggested by Heaton (1990). This suggests that the rate-dependent healing mechanism could be one of several possible models. However, the rate- and state-friction law was originally proposed (*e.g.* Dieterich, 1981; Ruina, 1983) to account for laboratory experimental data on rock friction at very low slip-

rates ranging between 10^{-6}-10^{-3} cm/s, but its extrapolation to higher slip velocities (10^1-10^2 cm/s) in the dynamic rupture process of actual earthquakes still does not seem justifiable.

The preliminary results for the Morgan Hill earthquake indicate, however, that the dynamic rupture model involving heterogeneous dynamic stress drop with the existence of barriers of high strength excess could equally well account for the short rise times. The above evidence would imply that the heterogeneous distribution of shear stress and fault strength introduces shorter length scales of fault segmentation and hence could produce short slip durations. It would follow that in this case a simple, critical stress fracture criterion together with a velocity-independent sliding friction could well explain the dynamic rupture process.

5. Summary

As described in some detail, several attempts have been made in the last few years to recover the dynamic rupture processes of large to moderate-size, inter-plate and intraplate earthquakes. The present paper reviews these approaches, summarizes some of the results, and discusses their tectonic implications.

Two approaches have been applied to date. One is to infer the dynamic model including the spatial distribution of the dynamic stress drop and strength excess on the fault, from the distribution of slip and rupture times previously obtained from kinematic waveform inversion. The other is to apply kinematic waveform inversion and dynamic crack inversion alternately to derive the above four kinematic and dynamic parameters simultaneously, by obtaining a best fit between the synthetic and recorded waveforms.

These studies have revealed heterogeneous distribution of dynamic stress drop up to 150 bars and strength excess of several tens of bars for some of the earthquakes. In two strike-slip California earthquakes, negative stress drops down to −20 bars were identified in a shallow section of the fault. This suggests that there could be a zone of velocity-strengthening frictional behavior in the shallower part of the crust. The dynamic models yielded quite short rise times comparable to those inferred from kinematic modeling of ground motion data. The short slip durations for these earthquakes may probably be attributed to shorter length scale due to the heterogeneities of shear stress and fault strength.

Acknowledgements

REFERENCES

ARCHULETA, R.J. (1984): A faulting model for the 1979 Imperial Valley earthquake, *J. Geophys. Res.*, **89**, 4559-4585.

BEROZA, G.C. and P. SPUDICH (1988): Linearized inversion for fault rupture behavior: application to the 1984, Morgan Hill, California, earthquake, *J. Geophys. Res.*, **93**, 6275-6296.

BLANPIED, M.L., D.A. LOCKNER and J.D. BYERLEE (1991): Fault stability inferred from granitesliding experiments at hydrothermal conditions, *Geophys. Res. Lett.*, **18**, 609-612.

BOATWRIGHT, J. and H. QUIN (1986): The seismic radiation from a 3-D dynamic model of a complex rupture process. Part I: confined ruptures, in *Earthquake Source Mechanics*, edited by S. DAS, J. BOATWRIGHT and C. SCHOLZ, Am. Geophys. Union, 97-109.

COCHARD, A. and R. MADARIAGA (1994): Dynamic faulting under rate-dependent friction, *PAGEOPH*, **142**, 419-445.

DAS, S. (1981): Three-dimensional spontaneous rupture propagation and implication for the earthquake source mechanism, *Geophys. J. R. Astr. Soc.*, **67**, 375-393.

DAS, S. and K. AKI (1977): A numerical study of two-dimensional spontaneous rupture propagation, *Geophys. J.R. Astr. Soc.*, **50**, 643-668.

DAY, S.M. (1982): Three-dimensional simulation of spontaneous rupture: the effect of non-uniform prestress, *Bull. Seismol. Soc. Am.*, **72**, 1881-1902.

DIETERICH, J.H. (1981): Constitutive properties of faults with simulated gouge in mechanical behavior of crustal rocks, edited by N.L. CARTER, M. FRIEDMAN, J.M. LOGAN

and D.W. Stearns, Am. Geophys. Union, *Geophys. Monogr. Ser.*, **24**, 103-120.

Fukuyama, E. (1991): Inversion for the rupture details of the 1987 East Chiba earthquake, Japan, using a fault model based on the distribution of relocated aftershocks, *J. Geophys. Res.*, **96**, 8205-8217.

Fukuyama, E. and T. Mikumo (1993): Dynamic rupture analysis: Inversion for the source process of the 1990 Izu-Oshima, Japan earthquake (*M* 6.5), *J. Geophys. Res.*, **98**, 491-496.

Hartzell, S. (1989): Comparison of seismic waveform inversion results for the rupture history of a finite fault: application to the 1986 North Palm Springs, California earthquake, *J. Geophys. Res.*, **94**, 7515-7534.

Heaton, T.H. (1990): Evidence for the implications of self-healing pulses of slip in earthquake rupture, *Phys. Earth Planet. Inter.*, **64**, 1-20.

Horikawa, H. and K. Hirahara (1993): Retrieval of dynamic source parameters with waveform inversion, *EOS*, **74** (43), 400.

Ide, S. and M. Takeo (1944): the dynamic rupture process of the 1993 Kushiro-oki earthquake, *J. Geophys. Res.* (submitted).

Marone, C. and C.H. Scholz (1988): The depth of seismic faulting and the upper transition from stable to unstable slip regions, *Geophys. Res. Lett.*, **15**, 621-624.

Mikumo, T. (1992): Dynamic fault rupture and stress recovery processes in continental crust under depth-dependent shear strength and frictional parameters, *Tectonophysics*, **211**, 201-222.

Mikumo, T. and T. Miyatake (1978): Dynamical rupture process on a three-dimensional frictional fault with non-uniform frictions and near-field seismic waves, *Geophys. J.R. Astr. Soc.*, **54**, 417-438.

Mikumo, T., K. Hirahara and T. Miyatake (1987): Dynamic fault rupture processes in heterogeneous media, *Tectonophysics*, **144**, 19-36.

Mikumo, T. and T. Miyatake (1993): Dynamic rupture processes on a dipping fault, and estimates of stress drop and strength excess from the results of waveform inversion, *Geophys. J. Int.*, **112**, 481-496.

Mikumo, T. and T. Miyatake (1994): Heterogeneous distribution of dynamic stress drop and relative fault strength recovered from the results of waveform inversion: the 1984 Morgan Hill, California earthquake,

Bull. Seismol. Soc. Am. (in press).

Mikumo, T. and G. Beroza (1994): Dynamically consistent inversion of strong motion data for the 1984 Morgan Hill, California, earthquake, presented at the *1994 IASPEI meeting, Wellington*.

Miyatake, T. (1980): Numerical simulations of earthquake source process by a three-dimensional crack model. Part I: rupture process, *J. Phys. Earth*, **28**, 565-598.

Miyatake, T. (1992a): Reconstruction of dynamic rupture process of an earthquake with constraints of kinematic parameters, *Geophys. Res. Lett.*, **19**, 349-352.

Miyatake, T. (1992b): Dynamic rupture processes of inland earthquakes in Japan: weak and strong asperities, *Geophys. Res. Lett.*, **19**, 1041-1044.

Miyatake, T. (1993): Dynamic fault rupture processes derived from the waveform inversion (7), *Abstr. Seismol. Soc. Japan* (in Japanese), n. 2, 342.

Quin, H. (1990): Dynamic stress drop and rupture dynamics of the October 15, 1979 Imperial Valley, California earthquake, *Tectonophysics*, **175**, 93-117.

Ruina, A.L. (1983): Slip instability and state variable friction laws, *J. Geophys. Res.*, **88**, 10359-10370.

Scholz, C.H. (1990): *The Mechanics of Earthquakes and Faulting* (Cambridge Univ. Press, Cambridge), pp. 439.

Stesky, R.M. (1978): Mechanism of high temperature frictional sliding in Westerly granite, *Can. J. Earth Sci.*, **15**, 361-375.

Takeo, M. (1987): An inversion method to analyze the rupture process of earthquake using near-field seismograms, *Bull. Seismol. Soc. Am.*, **77**, 490-513.

Takeo, M. (1988): Rupture process of the 1980 Izu-Hanto-Oki earthquake deduced from strong motion seismograms, *Bull. Seismol. Soc. Am.*, **78**, 1074-1091.

Takeo, M. and N. Mikami (1987): Inversion of strong motion seismograms for the source process of the Nagano-Ken-Seibu earthquake of 1984, *Tectonophysics*, **144**, 271-285.

Takeo, M. and N. Mikami (1990): Fault heterogeneity of inland earthquakes in Japan, *Bull. Earthq. Res. Inst.*, **65**, 541-569.

Yomogida, K. and T. Nakata (1994): Large slip velocity of the surface ruptures associated with the 1990 Luzon Earthquake, *Geophys. Res. Lett.*, **21**, 1799-1802.